Phytopathology Research

RESEARCH

Open Access

Synthetic modulation of ROS scavenging during host—*Sclerotinia sclerotiorum* interaction: a new strategy for the development of highly resistant plants

Yijuan Ding[1,2,3†], Baoqin Yan[1,4†], Siqi Zhao[1,2,3], Yangui Chen[1,2,3], Huafang Wan[1,2,3] and Wei Qian[1,2,3*]

Abstract

Sclerotinia sclerotiorum is a widespread fungal pathogen responsible for significant crop losses across the globe. The challenge of breeding resistant varieties is exacerbated by the fungus's sophisticated pathogenic mechanisms. A pivotal factor in the host-pathogen interaction is the regulation of reactive oxygen species (ROS) within both the fungi and the host plants. However, there is currently no efficient strategy to leverage this interaction mechanism for developing disease-resistant crop varieties. Here, we introduce an engineered ROS scavenging system designated as syn-ROS for impairing ROS neutralization in *S. sclerotiorum* while concurrently fortifying it in the host. The syn-ROS system comprises gene silencing constructs targeting the *S. sclerotiorum* Cu/Zn superoxide dismutase (*SsSOD*) and its copper chaperone (*SsCCS*), alongside overexpression constructs for the *Arabidopsis thaliana AtSOD1* and *AtCCS*. Transgenic plants carrying the syn-ROS system demonstrated a marked enhancement in resistance to *S. sclerotiorum*. Upon infection, the expression of *SsSOD* and *SsCCS* was reduced, while the expression of *AtSOD1* and *AtCCS* was enhanced in syn-ROS transgenic plants. Moreover, the infected syn-ROS plants showed decreased Cu/Zn SOD enzyme activity and elevated ROS concentrations within the fungal cells. In contrast, the cells of *A. thaliana* manifested increased Cu/Zn SOD enzyme activity and lowered ROS levels. Collectively, these findings suggest a novel and promising approach for contriving plants with robust resistance by synthetically manipulating ROS scavenging activities in the interaction between the host and *S. sclerotiorum*.

Keywords *CCS*, ROS scavenging, Resistant, *Sclerotinia sclerotiorum*, *SOD*, Synthetic

Background

Sclerotinia sclerotiorum is a phytopathogen with a broad host range, inflicting significant damage to vital food crops (Bolton et al. 2006; Liang and Rollins 2018). The ability of this pathogen to produce durable sclerotia complicates its management and underscores the intricacy of its pathogenic mechanisms (Zhu et al. 2013). Despite numerous attempts to mitigate its impact, the existing control strategies for *S. sclerotiorum* fall short, highlighting the imperative to devise innovative management approaches that effectively curb its damage. An in-depth comprehension of the interaction between the host

†Yijuan Ding and Baoqin Yan contributed equally to this work.

*Correspondence:
Wei Qian
qianwei666@hotmail.com
[1] Integrative Science Center of Germplasm Creation in Western China (CHONGQING) Science City and Southwest University, College of Agronomy and Biotechnology, Southwest University, Chongqing 400715, China
[2] Academy of Agricultural Sciences, Southwest University, Chongqing 400715, China
[3] Engineering Research Center of South Upland Agriculture, Ministry of Education, Chongqing 400715, China
[4] Academy of Agricultural Sciences, Gansu 744000, China

plants and *S. sclerotiorum* could pave the way for developing novel control methods to combat Sclerotinia stem rot.

S. sclerotiorum secretes an arsenal of plant cell wall-degrading enzymes (PCWDEs), cutinase, proteases, and oxalic acid (OA), along with various effectors to facilitate the destruction of host cells and enable the pathogen to manipulate the host's cellular processes (Williams et al. 2011; Liang and Rollins 2018). In a defensive countermeasure, plants have evolved a sophisticated two-layered immune surveillance system to thwart pathogenic attacks (Jones and Dangl 2006). Pattern recognition receptors (PRRs) at the cell surface detect conserved pathogen-associated molecular patterns (PAMPs), thereby initiating PAMP-triggered immunity (PTI). Pathogens deploy effectors to subvert this frontline defense, activating effector-triggered immunity (ETI). The defenses mounted by PTI and ETI share common downstream immune responses, orchestrating a comprehensive protective strategy (Boller and Felix 2009). Recent findings underscore the importance of a prompt and initial plant defense involving the transient generation of reactive oxygen species (ROS), a crucial aspect of PTI and ETI (Yuan et al. 2021). Contemporary studies also illustrate the pivotal role of modulating ROS accumulation during host-pathogen interactions (Singh et al. 2021). *S. sclerotiorum* is known to finely tune the host's redox environment, dampening the oxidative burst during the early stages of infection to benefit its proliferation while inducing ROS levels in the late stages of infection to promote apoptotic cell death and facilitate disease progression (Williams et al. 2011; Kabbage et al. 2013).

ROS, such as singlet oxygen, superoxide anion ($\cdot O^{2-}$), hydrogen peroxide (H_2O_2), and hydroxyl anion, play a pivotal role in directly neutralizing pathogens and blocking their incursions (Mittler 2017). Moreover, ROS serve as signaling molecules that prompt the activation of defense gene expression and initiate immune responses in plants (Mittler et al. 2011; Waszczak et al. 2018). To overcome the ROS onslaught from the host and ensure successful colonization, fungal phytopathogens have developed sophisticated ROS scavenging strategies to shield themselves from ROS-induced damage (Singh et al. 2021). The ROS defense apparatus within fungi has been thoroughly investigated (Segal and Wilson 2018). A suite of antioxidant enzymes, including superoxide dismutase (SOD), catalase (CAT), peroxidases (POD), thioredoxins (Trx), and glutaredoxins (GSH), along with a variety of non-enzymatic antioxidants, is central to the intracellular detoxification of ROS (Shao et al. 2020). SOD acts as the chief converter of superoxide radicals, mitigating the hazardous excess of ROS (Mittler 2017). Experimental evidence in the phytopathogenic fungus *S. sclerotiorum* reveals that suppressing *SsSOD* expression correlates with reduced fungal aggressiveness (Veluchamy et al. 2012; Xu and Chen 2013). Our prior research indicated that *S. sclerotiorum* enhances the copper chaperone gene *SsCCS* expression to activate *SsSOD*, a crucial step for the fungus to counteract high ROS levels during infection and maintain viability (Ding et al. 2020). Similarly, the induction of CCS (copper chaperone for SOD) in resistant host plants is instrumental in preserving the antioxidative function of SOD, thus mitigating excess ROS (Ding et al. 2020).

In the current study, we engineered a novel synthetic ROS scavenging system by introducing RNA interference (RNAi) constructs targeting the *S. sclerotiorum* genes *SsSOD* and *SsCCS*, as well as overexpression vectors for the *A. thaliana* genes *AtSOD1* and *AtCCS*. Our results demonstrate that plants equipped with this synthetic system showed enhanced resistance against *S. sclerotiorum*. Through comprehensive analysis, we concluded that the observed increase in resistance was principally due to the dual effect of impaired ROS detoxification in *S. sclerotiorum* and augmented ROS scavenging capacity in *A. thaliana* during the course of infection.

Results

A synthetic ROS scavenging system was designed and successfully established in *A. thaliana*

Our previous research elucidated the role of SOD and CCS in the modulation of ROS in both the fungus and host plants during *S. sclerotiorum* infection (Ding et al. 2020). In this present study, *SOD* and *CCS* genes from *A. thaliana* and *S. sclerotiorum* were selected to construct the synthetic ROS scavenging system. Expression analysis indicated a significant elevation in the expression levels of *SsSOD* and *SsCCS* amidst infection (Additional file 1: Figure S1). Among the three *SOD* homolog genes in *A. thaliana*, *AtSOD1* showed the highest expression level during *S. sclerotiorum* infection (Additional file 1: Figure S1). Concurrently, an infection-induced upsurge was observed for *AtCCS* (Additional file 1: Figure S1). Phylogenetic tree analyses confirmed the distinctiveness of *SsCCS* and *SsSOD* from plant CCS and SODs, respectively (Additional file 1: Figure S2). Multiple sequence alignment showed that the target RNAi sequence of *SsSOD* revealed 17.43% similarity with *AtSOD1*, and the target RNAi sequence of *SsCCS* revealed 7.17% similarity with *AtCCS* (Additional file 1: Figure S3). Specific sequences of *SsSOD* and *SsCCS* were used to construct single-target Host-induced Gene Silencing (HIGS) binaries (*SsSOD*-HIGS and *SsCCS*-HIGS) and a double-target HIGS binary (*SsCCS-SsSOD*-HIGS) (Fig. 1a). To enhance ROS detoxification in *A. thaliana* during infection, single (*AtCCS*-OE and *AtSOD1*-OE) and double-target

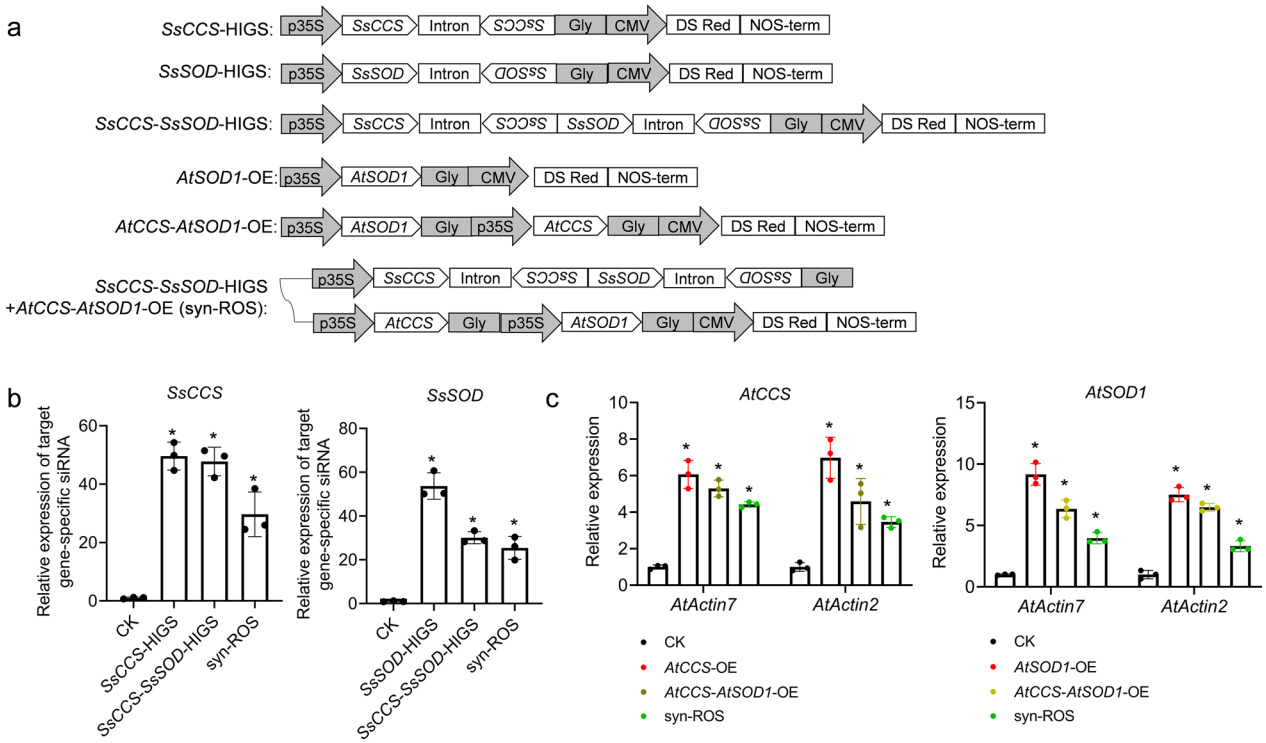

Fig. 1 Identification and verification of transgenic *A. thaliana* plants carrying the reactive oxygen species (ROS) scavenging system binary vectors. **a** Schematic representation of the binary vectors used for molecular design of ROS scavenging. **b** Relative expression levels of specific siRNA targets for *SsCCS* and *SsSOD* in transgenic *A. thaliana* plants. The expression levels were quantified by normalizing the quantity of *A. thaliana AtU6-26* cDNA in different samples. **c** Relative expression levels of *AtCCS* and *AtSOD1* in transgenic *A. thaliana* plants. The expression levels were quantified by normalizing the quantity of *A. thaliana AtActin7* and *AtActin2* cDNA in different samples. Data are presented as means ± SEM (n = 3, technical replicates). Asterisks indicate a statistically significant difference with the control line (CK) at $p < 0.05$ (two-sided Student's *t*-test). The relative expression of target siRNA or gene in CK was set as one, respectively. CK: *A. thaliana* plants carrying the empty vector

(*AtCCS-AtSOD1*-OE) overexpression binaries for *AtCCS* and *AtSOD1* were constructed (Ding et al. 2020, Fig. 1a). The synthetic ROS scavenging system (syn-ROS: *SsCCS-SsSOD*-HIGS + *AtCCS-AtSOD1*-OE) was engineered by fusing *SsCCS-SsSOD*-HIGS with *AtCCS-AtSOD1*-OE, aiming to preemptively mitigate the ROS neutralizing capacity in *S. sclerotiorum* while concurrently reinforcing it within *A. thaliana* during the infection process (Fig. 1a).

All the binary vectors were transformed into wild-type *A. thaliana* Col-0. The T_3 generation transgenic seedlings showed no noticeable difference in growth compared to control plants carrying the empty vector (Additional file 1: Figure S4). To confirm the efficiency of HIGS, stem-loop qRT-PCR was conducted to measure the production of specific siRNAs for *SsCCS* (*SsCCS*-siRNA) and *SsSOD* (*SsSOD*-siRNA). The results revealed high expression of *SsCCS*-siRNA in *SsCCS*-HIGS, *SsCCS-SsSOD*-HIGS, and syn-ROS lines, while *SsSOD*-siRNA was highly expressed in *SsSOD*-HIGS, *SsCCS-SsSOD*-HIGS, and syn-ROS lines (Fig. 1b). No expression of *SsCCS*-siRNA and *SsSOD*-siRNA was detected in control plant (Fig. 1b). To investigate the expression of the host genes, qRT-PCR analysis, normalized to the reference genes *AtActin7* and *AtActin2*, revealed that the transcript levels of *AtCCS* in *AtCCS*-OE, *AtCCS-AtSOD1*-OE, and syn-ROS lines experienced an average increase of 6.5-fold, 4.9-fold, and 3.9-fold, respectively, compared to the controls (Fig. 1c). Similarly, transcript abundance of *AtSOD1* in *AtSOD1*-OE, *AtCCS-AtSOD1*-OE, and syn-ROS lines was averagely escalated to 8.3-fold, 6.4-fold, and 3.6-fold above control levels, respectively (Fig. 1c). Furthermore, we analyzed the gene expression of *AtCCS* and *AtSOD1* in HIGS lines, and no significant difference was detected among CK (control line) and HIGS lines (Additional file 1: Figure S5).

Enhanced *S. sclerotiorum* resistance was observed in plants harboring the synthetic ROS scavenging system

To evaluate the effectiveness of the synthetic ROS scavenging system in protecting transgenic *A. thaliana* plants from *S. sclerotiorum* infection, resistance was assessed using both in vitro (detached leaf) and in vivo (intact leaf) assays. The results revealed that the lesion sizes on

the infected transgenic lines were notably smaller than those on the control line at 24 hpi (hours post-inoculation) (Fig. 2a, b). In the in vitro assay, the average lesion size on the control line was 1.00 cm^2. The lesions were significantly reduced by approximately 46.48% to 73.00% on the transgenic lines, specifically *SsCCS*-HIGS (0.54 cm^2), *SsSOD*-HIGS (0.41 cm^2), *SsCCS-SsSOD*-HIGS (0.38 cm^2), *AtCCS*-OE (0.51 cm^2), *AtSOD1*-OE (0.41 cm^2), *AtCCS-AtSOD1*-OE (0.33 cm^2), and syn-ROS line (0.27 cm^2) (Fig. 2c). Additionally, compared to the lines harboring single or dual gene constructs (*SsCCS*-HIGS, *SsSOD*-HIGS, *SsCCS-SsSOD*-HIGS, *AtCCS*-OE, *AtSOD1*-OE, and *AtCCS-AtSOD1*-OE), the lesion sizes on the syn-ROS line displayed further reductions for 49.56%, 33.52%, 22.33%, 47.57%, 34.53%, and 17.67%, respectively (Fig. 2c). Similar results were recorded in the in vivo assay. On the intact leaves, the syn-ROS line showed a striking reduction in lesion size of approximately 70.24% (0.24 cm^2), compared to the control line (0.95 cm^2) (Fig. 2d). Moreover, when contrasted with the lines carrying single or dual gene constructs, the lesions on the syn-ROS line were decreased by 53.98%, 39.19%, 35.13%, 50.90%, 38.94%, and 26.17% for *SsCCS*-HIGS, *SsSOD*-HIGS, *SsCCS-SsSOD*-HIGS, *AtCCS*-OE, *AtSOD1*-OE, and *AtCCS-AtSOD1*-OE, respectively (Fig. 2d). These findings highlight the potential benefits of employing synthetic ROS scavenging systems for enhancing resistance to *S. sclerotiorum* in *A. thaliana*.

The expression levels of target genes during *S. sclerotiorum* infection in transgenic *A. thaliana* were quantified

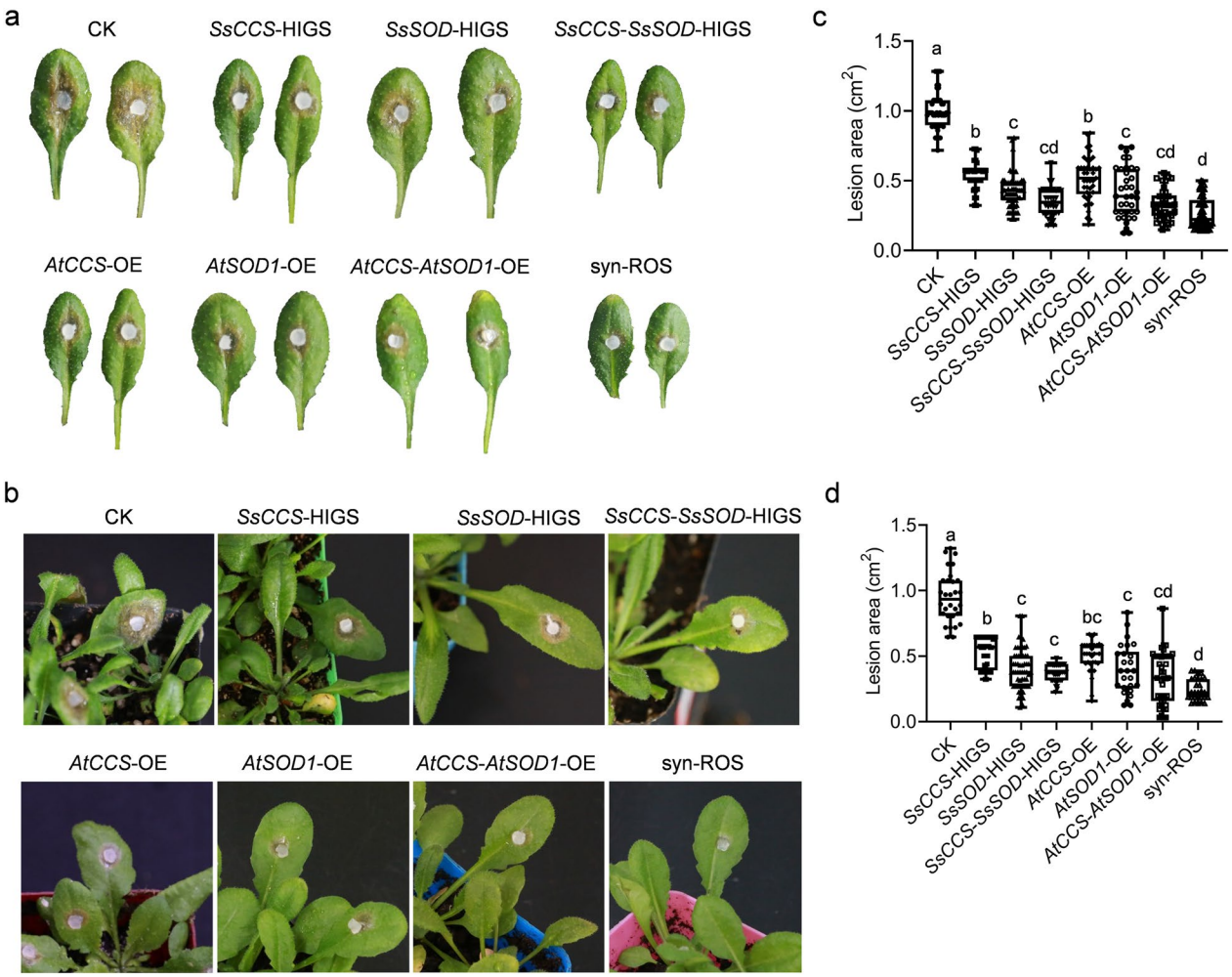

Fig. 2 Lesion areas of transgenic *A. thaliana* plants infected with *Sclerotinia sclerotiorum* at 24 h post-inoculation (hpi). **a** and **b** Disease symptoms of transgenic *A. thaliana* plants at 24 hpi with *S. sclerotiorum* wild-type strain 1980 in vitro and in vivo. **c** and **d** Quantification of lesion areas at 24 hpi in vitro and in vivo. Data are presented as means ± SEM (n > 15 plants). Different letters indicate significant difference at $p < 0.05$ (one-way ANOVA followed by Tukey's post hoc test). CK: *A. thaliana* plants carrying the empty vector

at 12 and 24 hpi utilizing the qRT-PCR assay. Notable reductions in the relative gene expression of *SsCCS* and *SsSOD* were detected in the transgenic lines *SsCCS*-HIGS, *SsSOD*-HIGS, *SsCCS-SsSOD*-HIGS, and syn-ROS lines in comparison to the control line (Fig. 3a, b). After normalizing with two internal housekeeping genes (*SsTubullin* and *SsActin*), the transcript levels of *SsCCS* exhibited a mean down-regulation of roughly 61%, 50%, and 29% in the *SsCCS*-HIGS, *SsCCS-SsSOD*-HIGS, and syn-ROS lines at 12 hpi, respectively (Fig. 3a). At 24 hpi, this down-regulation increased to about 64%, 60%, and 58%, respectively (Fig. 3a). Similarly, down-regulation was observed for *SsSOD* in the *SsSOD*-HIGS, *SsCCS-SsSOD*-HIGS, and syn-ROS lines (Fig. 3b), where the average transcript levels showed a decrease in expression by approximately 43% for both the *SsSOD*-HIGS

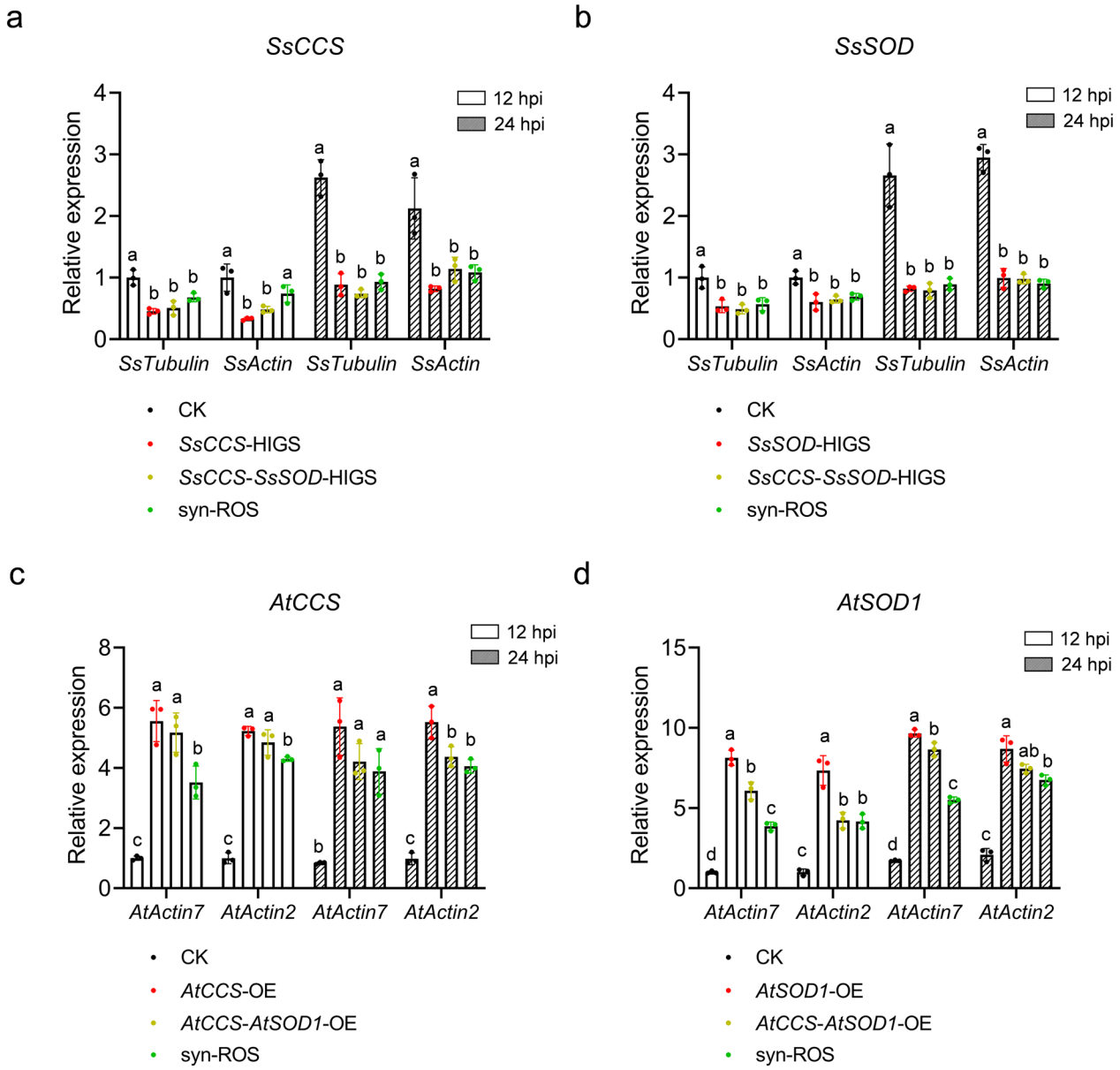

Fig. 3 Gene expression analysis in transgenic *A. thaliana* plants during infection. **a**–**d** Relative expression levels of *SsCCS*, *SsSOD*, *AtCCS*, and *AtSOD1* in transgenic *A. thaliana* plants at 12 hpi and 24 hpi. The expression levels were quantified by normalizing the quantity of *S. sclerotiorum Sstubulin* and *SsActin* cDNA for *SsCCS* and *SsSOD*, and *A. thaliana AtActin7* and *AtActin2* cDNA for *AtCCS* and *AtSOD1* in different samples. Data are presented as means ± SEM (n = 3, technical replicates). Different letters indicate significant difference at $p < 0.05$ (one-way ANOVA followed by Tukey's post hoc test). The relative expression of the target gene in CK at 12 hpi was set as one, respectively. CK: *A. thaliana* plants carrying the empty vector

and *SsCCS-SsSOD*-HIGS, and 37% for the syn-ROS lines at 12 hpi, with a more pronounced reduction of 67%, 68%, and 68% at 24 hpi, respectively (Fig. 3b). Conversely, the relative expression of *AtCCS* and *AtSOD1* displayed an upward trend during the infection in the *AtCCS*-OE, *AtSOD1*-OE, *AtCCS-AtSOD1*-OE, and syn-ROS lines when compared to the control line (Fig. 3c, d). After normalization with two internal reference genes (*AtActin7* and *AtActin2*), the transcript levels of *AtCCS* were, on average, approximately 5.4-fold, 5.0-fold, and 3.9-fold higher in the *AtCCS*-OE, *AtCCS-AtSOD1*-OE, and syn-ROS lines at 12 hpi, respectively (Fig. 3c). This elevation in gene expression persisted at 24 hpi, where it rose to about 6.0-fold, 4.7-fold, and 4.4-fold, respectively (Fig. 3c). Similarly, the average transcript levels of *AtSOD1* revealed a surge in expression by roughly 7.7-fold, 5.2-fold, and 4.0-fold at 12 hpi, and by 4.8-fold, 4.3-fold, and 3.2-fold at 24 hpi in the *AtSOD1*-OE, *AtCCS-AtSOD1*-OE, and syn-ROS lines, respectively (Fig. 3d). These findings elucidate that the synthetic ROS scavenging system in *A. thaliana* effectively attenuates the expression of pathogenic genes *SsCCS* and *SsSOD* while concurrently amplifying the plant *AtCCS* and *AtSOD1*, during an encounter with *S. sclerotiorum*, thus impeding the expansion of *S. sclerotiorum*.

ROS accumulation in *S. sclerotiorum* cells and *A. thaliana* cells

To investigate the functionality of the synthetic ROS scavenging system further, we assessed ROS accumulation and Cu/Zn SOD enzyme activity in *S. sclerotiorum*-infected transgenic *A. thaliana* lines during infection. ROS accumulation was determined using DAB (3,3′-diaminobenzidine) and NBT (Nitroblue tetrazolium chloride) staining at 24 hpi. The results indicated pronounced staining in the control line, indicative of higher ROS levels, while the syn-ROS line displayed markedly less staining (Fig. 4a). This observation was substantiated by quantifying H_2O_2 and $\cdot O^{2-}$ levels, with the infected syn-ROS line demonstrating lower H_2O_2 and $\cdot O^{2-}$ content relative to the control line (Fig. 4b, c). Furthermore, an elevated $\cdot O^{2-}$ level was noted in the lesion area of the *SsCCS-SsSOD*-HIGS line compared to the control, hinting at an impaired ROS scavenging capability in *S. sclerotiorum* (Fig. 4a, c).

To monitor the dynamic ROS levels in *A. thaliana* and *S. sclerotiorum* cells, we analyzed the gene expression of cytosolic thiol peroxidase, a known intracellular sensor for ROS (Delaunay et al. 2002; Bi et al. 2022), from *A. thaliana* (*AtPRXIIB*) and *S. sclerotiorum* (*SsGpx3*). Our findings revealed a down-regulation of *AtPRXIIB* expression in the syn-ROS line (Fig. 4d). Conversely, *SsGpx3* expression was up-regulated in the syn-ROS line in comparison to the control (Fig. 4e) at 24 hpi. Furthermore, after isolating cells from the infected tissue at the same time point, we assessed the ROS levels in both *S. sclerotiorum* and *A. thaliana* cells using H_2DCFDA (2′,7′-dichlorodihydrofluorescein diacetate) staining (Fig. 4f, g). In comparison with those of the control line, fluorescence microscopy analyses showed a decrease in ROS levels in *A. thaliana* cells of the syn-ROS line (Fig. 4f, h), whereas *S. sclerotiorum* cells of the syn-ROS line exhibited an increase (Fig. 4g, h). These findings align with the Cu/Zn SOD enzyme activity results, where a significantly lower activity was detected in *S. sclerotiorum* cells, and a higher activity was observed in *A. thaliana* cells from the infected syn-ROS line compared to the control line (Fig. 5).

In summary, the data suggest that the syn-ROS system augments ROS detoxification within the host plant while concurrently inhibiting fungal ROS detoxification mechanisms. This imbalance restricts the ability of *S. sclerotiorum* to adapt to the host's hyperoxic conditions and leads to a decrease in the pathogen's virulence in transgenic plants.

Discussion

The growing prevalence of fungicide resistance compounds the escalating threat of fungal phytopathogens to global crop yields. Tackling this issue necessitates an in-depth understanding of the mechanisms by which crop plants resist fungal infections and the strategies fungi employ to colonize their hosts. These insights are essential for developing crops with broad-spectrum disease resistance (Zhao et al. 2022). In our study, we engineered a molecular synthetic pathway aimed at bolstering the plant's defensive mechanisms while concurrently inhibiting fungal pathogenic processes. We specifically targeted the ROS scavenging pathway to test the effectiveness of our design against *S. sclerotiorum*. The engineered transgenic *A. thaliana* with the synthetic ROS scavenging system displayed significantly increased resistance to *S. sclerotiorum*, underscoring the potential of our approach. These results enhance our comprehension of plant-pathogen interaction and offer practical applications for the management of crop diseases.

Traditionally, the overexpression of resistance genes has proven to be a successful strategy against *S. sclerotiorum* in a variety of crops. Resistance has been achieved by overexpressing genes, such as *BnaMPK3*, *BnaMPK6*, *BnPGIPs*, and various others in crops like *Brassica napus*, and introducing genes from different species, such as barley oxalate oxidase OXO into *Brassica juncea* and lettuce, as well as the leveraging of different resistance genes in soybean and tobacco (Yang et al. 2019; Wang et al. 2019, 2020a, b; Liu et al. 2021; Peng et al. 2021; Verma and Kaur

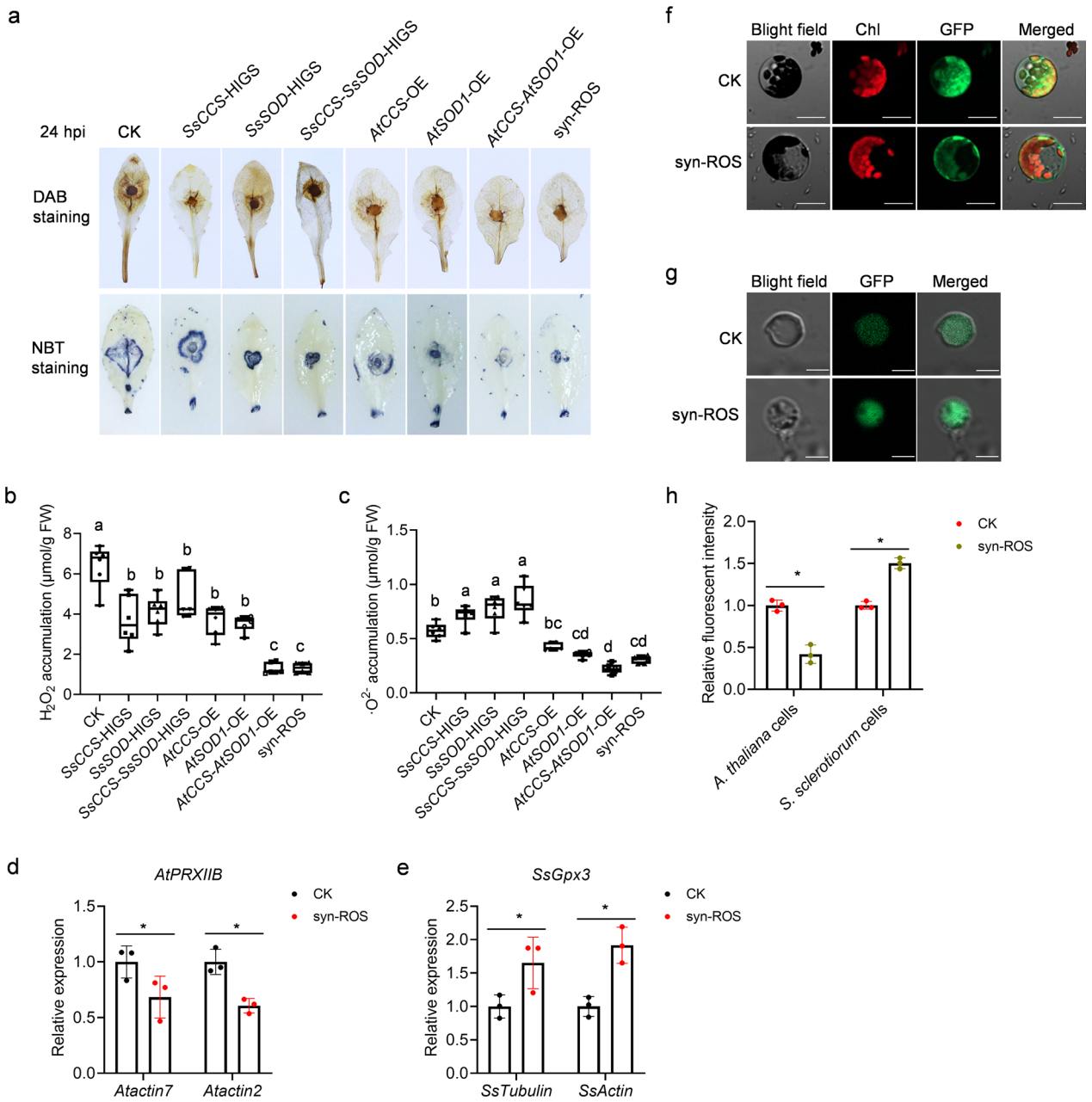

Fig. 4 Reactive oxygen species (ROS) accumulation in infected transgenic *A. thaliana* plants. **a** 3,3′-diaminobenzidine (DAB, indicating H_2O_2 accumulation) and nitroblue tetrazolium (NBT, indicating superoxide anion [$\cdot O^{2-}$] accumulation) staining at 24 hpi. One representative replicate from the three independent experiments is shown. Three leaves were stained in each experiment. **b** and **c** Quantification of H_2O_2 accumulation and $\cdot O^{2-}$ accumulation in the infected tissue (necrotic tissue including the tissue 0.5 cm around the lesion edge) of transgenic *A. thaliana* plants. Data are presented as means ± SEM (n = 6, independent experiments). **d** Relative expression level of *AtPRXIIB* in syn-ROS and control lines at 24 hpi by normalizing with the quantity of *A. thaliana AtActin7* and *AtActin2* cDNA. Data are presented as means ± SEM (n = 3, technical replicates). The relative expression of the target gene in CK was set as one. **e** Relative expression level of *SsGpx3* in syn-ROS and control lines at 24 hpi by normalizing with the quantity of *S. sclerotiorum Sstubulin* and *SsActin* cDNA. Data are presented as means ± SEM (n = 3, technical replicates). The relative expression of the target gene in CK was set as one. **f** ROS accumulation in *A. thaliana* protoplasts of infected syn-ROS and control lines at 24 hpi as detected by the fluorescent probe 2′,7′-dichlorofluorescein diacetate (H_2DCFDA). Scale bars = 20 μm. **g** ROS accumulation in *S. sclerotiorum* protoplasts of infected syn-ROS at 24 hpi as detected by the fluorescent probe H_2DCFDA. Scale bars = 5 μm. **h** Quantification of relative fluorescent intensity in **f** and **g**. Data are presented as means ± SEM (n = 3, independent experiments). The fluorescent images of the protoplasts were captured using a confocal microscope. Different letters and asterisks indicate significant difference at $p < 0.05$ (**b** and **c**, one-way ANOVA followed by Tukey's post hoc test; **d**–**h**, two-sided Student's *t*-test). CK: *A. thaliana* plants carrying the empty vector

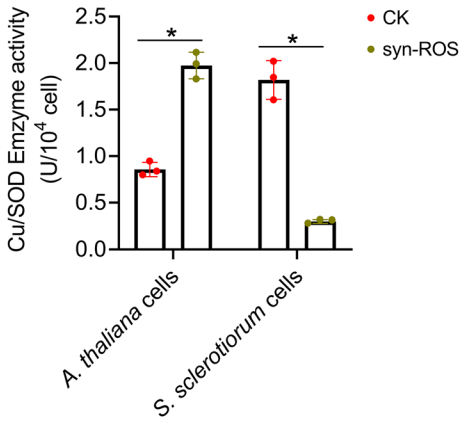

Fig. 5 Copper/zinc superoxide dismutase (Cu/Zn SOD) enzyme activity in *S. sclerotiorum* cells and *A. thaliana* cells. Data are presented as means ± SEM (n = 3, independent experiments). Asterisks indicate a statistically significant difference at $p < 0.05$ (two-sided Student's *t*-test). CK: *A. thaliana* plants carrying the empty vector

2021; Wang et al. 2021; Zhang et al. 2021). Additionally, deploying HIGS, a technique utilizing RNA interference to target pathogens, has provided a novel method of conferring resistance in a range of host plants (Andrade et al. 2015; Ding et al. 2021; McCaghey et al. 2021; Maximiano et al. 2022; Rana et al. 2022; Wu et al. 2022). Our study has taken these efforts further by creating a genetic construct that simultaneously produces siRNAs aimed at suppressing the *SsSOD* and *SsCCS* genes of the pathogen and upregulating the expression of the plant's own *AtSOD1* and *AtCCS* genes. Transgenic *A. thaliana* lines harboring this construct (termed syn-ROS) demonstrated a substantial increase in resistance to *S. sclerotiorum* compared to control lines, with the syn-ROS line showing a marked twofold increase in resistance over those containing individual or dual-gene constructs. This signifies the success of our tailored molecular synthetic pathway in enhancing resistance to *S. sclerotiorum*.

The overabundance of ROS, often referred to as the oxidative burst, constitutes a pivotal component of the host-pathogen interaction. Upregulation of ROS-scavenging genes within the host has been associated with a bolstered defense against fungal infections instigated by a range of pathogens, including *Fusarium graminearum*, *Botrytis cinerea*, *Aspergillus niger*, and *S. sclerotiorum* (Koubaa and Brini 2020; Chai et al. 2022). Conversely, genetic deletion of SOD or catalase in various phytopathogens such as *Verticillium dahliae*, *B. cinerea*, *F. graminearum*, and *S. sclerotiorum*, elicits marked attenuation in lesion progression, host colonization efficiency, and pathogenic virulence (Veluchamy et al. 2012; Xu and Chen 2013; López-Cruz et al. 2017; Yao et al. 2016; Tian et al. 2021). This body of evidence suggests that strategic modulation of ROS scavenging enzymatic activity in both plant hosts and pathogens can converge upon a unified resistance phenotype in plants. Cu/Zn SOD, a metalloenzyme, is rendered active by copper ions that are translocated by the copper chaperone for SOD (CCS) (Banci et al. 2012). In our study, we observed a downregulation of *SsSOD* and *SsCCS* expression in the infected syn-ROS line, culminating in elevated ROS levels and diminished Cu/Zn SOD enzymatic activity within *S. sclerotiorum* cells. The transcript level of *AtSOD1* and *AtCCS* was increased in the syn-ROS lines, leading to a mitigation of ROS accumulation and an amplification of Cu/Zn SOD enzyme action. Our findings underscore the crucial significance of ROS equilibrium in governing host-pathogen interaction and intimate that targeted synthetic modulation of ROS levels could be harnessed in crop breeding strategies to maximize disease resistance.

ROS are pivotal signaling molecules that orchestrate a variety of vital biological functions, including the regulation of cellular proliferation and differentiation (Mittler 2017). In our investigation, we leveraged a synthetic ROS modulation pathway under the control of the CaMV 35S promoter, which facilitates constitutive and spatially variable expression across different tissues in transgenic lines (Kiselev et al. 2021). Despite these modifications, the transgenic seedlings of the T_3 generation did not display noticeable growth discrepancies when contrasted with control plants. One potential rationale for this observation lies in the capacity of SODs to transform radical species, such as superoxide and hydroxyl radicals, into molecular oxygen and H_2O_2. Subsequently, H_2O_2 is detoxified into H_2O and dioxygen by catalases and peroxidases (Mittler et al. 2011). These antioxidant defenses are pivotal in preserving ROS at baseline concentrations under normal physiological states in plants (El Hadrami et al. 2005). Moreover, the more pronounced signaling role of H_2O_2 as a principal secondary messenger may also explain the observed growth patterns (Sies et al. 2017). The balance between plant defense and growth presents a formidable challenge in current botanical research. Initiatives have been undertaken to uncover "molecular switch" promoters capable of activating the immune system exclusively upon pathogen assault, thus preventing activation under regular growth conditions, which could compromise plant development (Xu et al. 2017). Recent advancements identified an inducible promoter triggered by *S. sclerotiorum* that diminishes the inappropriate expression of defense genes (Lin et al. 2022). The application of such tailored "molecular switch" promoters may refine the construction of the synthetic molecular pathways examined in our analysis.

The insightful biological knowledge derived from fundamental research is poised to be translated into

practical advancements in plant breeding, as evidenced by recent studies (Yan and Wang 2023). The advent of molecular design breeding represents a sophisticated and precise method for crop enhancement that has become increasingly important in contemporary agriculture (Shen et al. 2019; Wang et al. 2020a, b). The methodology formulated in this investigation can be adapted to the molecular design of additional pathways beyond the regulation of ROS. Recent years have witnessed significant breakthroughs in comprehending the intricate interactions between host plants and the fungus *S. sclerotiorum*. A cadre of secreted proteins, such as SsSSVP1, SsCP1, SsITL, and SsPINE1, have been identified in directly interacting with host proteins to manipulate plant resistance pathways and, consequently, in heightening fungal virulence (Lyu et al. 2016; Yang et al. 2018; Tang et al. 2020; Wei et al. 2022). Deciphering the mechanisms of these interactions can facilitate the creation of *S. sclerotiorum*-resistant cultivars employing the strategy elucidated in our study.

Conclusions

This research introduces an innovative approach for combatting fungal pathogens, exemplifying a molecular synthetic pathway that modulates ROS detoxification. It underscores the burgeoning potential of employing targeted molecular design in precision breeding tactics.

Methods

Culture conditions for plants and fungal strains

The wild-type strain of *A. thaliana*, known as Col-0 (Columbia-0), was grown under long-day conditions, featuring a cycle of 16 h of light followed by 8 h of darkness in controlled-environment growth chambers set to 20°C. The wild-type strain of *S. sclerotiorum*, strain 1980, was regularly cultured and preserved on potato dextrose agar (PDA) plates, consisting of 20% potato, 2% dextrose, and 1.5% agar, at a temperature of 22°C.

Binary constructs and plant transformation

A 364 bp DNA fragment encoding *SsSOD* was utilized to construct the host-induced *SsSOD* silencing vector. The sense and antisense fragments were amplified using the primer pairs *SsSOD*-SF/SR and *SsSOD*-AF/AR, respectively (Additional file 2: Table S1). Similarly, to craft the host-induced *SsCCS* silencing vector, a 316 bp DNA fragment of *SsCCS* was used, with its sense and antisense sequences amplified using the primer pairs *SsCCS*-SF/SR and *SsCCS*-AF/AR, respectively (Additional file 2: Table S1). These sense and antisense sequences were subsequently linked in-frame to the 5' and 3' termini of an amiRNA stem-loop structure. These RNAi-based elements were cloned downstream of the 35S promoter in a vector marked with red fluorescence, yielding the RNAi-based host-induced gene silencing (HIGS) constructs *SsCCS*-HIGS and *SsSOD*-HIGS. To assemble the combined *SsCCS-SsSOD*-HIGS construct, the RNAi cassette for *SsCCS* (comprising sequence and antisense fragments with an intervening intron) was joined to the *SsSOD* RNAi cassette through an efficient process of homologous recombination using the ClonExpress II One Step Cloning Kit (Vazyme, Nanjing, China).

To create *AtCCS* and *AtSOD1* overexpression (OE) lines, the corresponding coding sequences for each gene were subcloned into a vector marked by red fluorescence and controlled by the 35S promoter. This resulted in the construction of the *AtCCS*-OE and *AtSOD1*-OE vectors. In assembling the dual overexpression construct *AtCCS-AtSOD1*-OE, the *AtCCS* overexpression cassette was fused with the *AtSOD1* overexpression cassette via homologous recombination.

A synthetic ROS scavenging construct was generated by merging the *SsCCS-SsSOD*-HIGS with the *AtCCS-AtSOD1*-OE cassettes through homologous recombination. The transformation of *A. thaliana* Col-0 plants with this construct was performed using the floral dip method (Clough and Bent 1998).

RNA isolation and transcript level analysis

Total RNA was extracted from the leaves of *A. thaliana* infected with the wild-type strain of *S. sclerotiorum* 1980 by employing the TRIzol method (Invitrogen, Carlsbad, CA). The extracted total RNA was then used to synthesize first-strand cDNA using the Evo M-MLV RT Kit with gDNA Clean for qPCR (Accurate Biotechnology Co, Hunan, China), following the manufacturer's instructions. Quantitative RT-PCR analyses were conducted on the Bio-Rad CFX96 Real-Time System (Bio-Rad, Hercules, CA, USA). The expression levels of *S. sclerotiorum* genes were analyzed using *SsTubulin* and *SsActin* as the internal controls, while expression levels for *A. thaliana* genes were determined using *AtActin7* and *AtActin2* for normalization. The real-time RT-PCR reactions utilized QuantiTect SYBR Green PCR Master Mix (Bio-Rad, USA), as specified by the manufacturer. The amplification program consisted of an initial cycle at 95 °C for 30 s, followed by 39 cycles at 95 °C for 5 s and 55–70 °C for 1 min. A melting curve analysis was then performed, ramping from 65 °C to 95 °C with a temperature increase of 0.5 °C every 5 s. Quantitative changes in gene expression were calculated using the $2^{-\Delta\Delta CT}$ method (Livak and Schmittgen 2001). The analysis incorporated data from three biological replicates per sample and was facilitated by CFX Manager™ software (version 3.0). Details of the primers employed in the real-time RT-PCR are enumerated in Additional file 2: Table S1.

sRNA detection

To detect the production of *SsCCS* and *SsSOD* siRNAs in transgenic *A. thaliana* plants, stem-loop qRT-PCR was performed against the *SsCCS* and *SsSOD* genes of *S. sclerotiorum*, following the protocol of Mahto et al. (2020), with some modifications. For this purpose, the 316 bp sequence of *SsCCS* and the 364 bp sequence of *SsSOD* used for constructing the RNAi-based HIGS vectors were employed for siRNA detection using the BLOCK-iT™ RNAi Designer (http://rnaidesigner.thermofisher.com/). Putative siRNA sequences (*SsCCS*: AACUUCCUCUCU CCCUCAUGUUC; *SsSOD*: UAAUCUGACUAUCUU CAACGG) were identified and selected for stem-loop qRT-PCR. Low molecular weight RNA was isolated and used to synthesize cDNA using the stem-loop primer (ST-*SsCCS* and ST-*SsSOD*). Stem-loop qRT-PCR was performed using the Bio-Rad CFX96 Real-Time System (Bio-Rad, Hercules, CA, United States) and SYBR Green PCR master mix (Bio-Rad, USA), following the manufacturer's instructions. The *A. thaliana* U6 gene (*AtU6-26*) was used as the internal reference to normalize the expression of siRNAs. The transcript levels of siRNAs were calculated from the threshold cycle using the $2^{-\Delta\Delta CT}$ method (Livak and Schmittgen 2001) with three replicates, and the data were analyzed using CFX Manager™ v3.0. The primers used for performing stem-loop qRT-PCR are listed in Additional file 2: Table S1.

Resistance assay

To evaluate resistance levels, mycelial plugs measuring 0.2 cm in diameter were excised from the active growth edges of the wild-type *S. sclerotiorum* strain 1980. These plugs were then inoculated on the transgenic *A. thaliana* plants according to the previously described procedure (Ding et al. 2020). The extent of infection was quantified by measuring the lesion areas at 24 hpi. Each experimental replicate included a minimum of five leaves from each plant line, and the experiments were replicated three times.

ROS accumulation assay

The evaluation of ROS accumulation in transgenic *A. thaliana* leaves was conducted using DAB and NBT staining, following the protocol of Kumar et al. (2014). The *A. thaliana* leaves were infiltrated with a DAB solution (pH 3.8, Solarbio) or an NBT solution (Solarbio) under a mild vacuum for a duration of five hours. Subsequently, the staining solution was exchanged for a bleaching solution with a composition of ethanol: acetic acid: glycerol in a ratio of 3:1:1. After approximately 15 min in a boiling water bath (~ 90–95 °C), the bleaching solution was replaced with the fresh bleaching solution, and the leaves were stained in 60% glycerin. The level of H_2O_2 and $\cdot O^{2-}$ in the infected tissue (necrotic tissue, including the tissue 0.5 cm around the lesion edge) of transgenic plants was quantified using the Hydrogen Peroxide (H_2O_2) content assay kit (BC3595; Solarbio) and Superoxide Anion activity content assay kit (BC1295; Solarbio), respectively, according to the manufacturer's protocol. The experiments were repeated six times.

To analyze the specific ROS scavenge ability in *S. sclerotiorum* and *A. thaliana* cells during infection, pure fungal and plant cells were isolated from infected *A. thaliana* tissue using the sequential protoplast purification method with modifications based on Cai et al. (2018). In brief, the infected *A. thaliana* tissue was rinsed with sterilized water to remove the hyphae on the surface of the leaves and then homogenized for one minute in isolation buffer (0.02 M MOPS buffer, pH 7.2, 0.2 M sucrose) using a blender on the highest speed setting to release *S. sclerotiorum* mycelium from host epidermal cells. The homogenate was filtered through a 70 µm nylon mesh to remove plant cell wall debris. The retained material on the filter was re-homogenized in an isolation buffer for 1 min and re-filtered. The resulting pellets were collected after centrifuging the pooled homogenate at 1500 *g* for 10 min, and then resuspended in 1% Triton X-100, washed three times with isolation buffer, and then incubated with plant cell wall digest solution (1.5% cellulose, 0.4% maceroenzyme, 0.4 M mannitol, 20 mM MES (pH 5.7), 20 mM KCl, 10 mM $CaCl_2$, and 0.1% BSA). After resuspension in 1% Triton X-100 and washing in isolation buffer five times to remove plant contents, the pellets were resuspended in lysing enzyme solution (2% lysing enzyme from *Trichoderma harzianum* (L3768, Sigma) and 0.2% snail enzyme from *Helix pomatia* (C8274, Sigma) in 0.8 M $MgSO_4$) and incubated at 28°C for 3–4 h to release fungal protoplasts. The fungal protoplasts were filtered through a 40 µm nylon mesh. *A. thaliana* cells were collected by digesting the retained plant material with plant cell wall digestion solution for 3 h at 25°C. The resulting plant protoplasts were filtered through a 70 µm nylon mesh.

Both purified fungal and plant cells were stained with H_2DCFDA (D6883, Sigma) to detect ROS contents. The fluorescent signal of H_2DCFDA staining reflects the ROS levels (Oparka et al. 2016). Samples were observed under a confocal microscope (LSM800/1080, Zeiss) with an excitation wavelength of 488 nm and an emission wavelength of 530 nm. To ensure consistency, the fluorescence intensity was compared across samples while maintaining uniform settings on the confocal microscope. Additionally, the enzyme activity of Cu/Zn superoxide dismutase (SOD) in the purified cells was determined using a Cu/Zn SOD assay kit (A001-4-1, Nanjing Jiancheng

Bioengineering Institute) according to the manufacturer's protocol. The experiments were repeated three times.

Statistical analysis

The experimental data accrued from the different biological replicates were analyzed using one-way analysis of variance (ANOVA). Subsequent statistical assessments were executed utilizing Prism 8 software (GraphPad Software, USA). The results were reported as the mean ± standard error of the mean (SEM). Differences achieving statistical significance when compared with the control were identified using a two-tailed Student's *t*-test, with * $P < 0.05$ denoting significance.

Abbreviations

ANOVA	Analysis of variance
CAT	Catalase
CCS	Copper chaperone for SOD
CK	Control line
Col-0	Columbia-0
DAB	3,3′-Diaminobenzidine
ETI	Effector-triggered immunity
GSH	Glutaredoxins
H_2DCFDA	2′,7′-Dichlorodihydrofluorescein diacetate
H_2O_2	Hydrogen peroxide
HIGS	Host-induced Gene Silencing
hpi	Hours-post inoculation
O^{2-}	Superoxide anion
OA	Oxalic acid
OE	Overexpression
OXO	Oxalate oxidase
PAMPs	Pathogen-associated molecular patterns
PCWDEs	Plant cell wall-degrading enzymes
PDA	Potato dextrose agar
POD	Peroxidases
PRRs	Pattern recognition receptors
PTI	PAMP-triggered immunity
RNAi	RNA interference
ROS	Reactive oxygen species
SEM	Standard error of the mean
SOD	Superoxide dismutase
syn-ROS	Synthetic ROS scavenging system
Trx	Thioredoxins
NBT	Nitroblue tetrazolium chloride

Supplementary Information

The online version contains supplementary material available at https://doi.org/10.1186/s42483-024-00238-9.

Additional file 1: Figure S1. Heat map depicting the expression levels of *SsCCS*, *SsSOD*, *AtCCS*, and *AtSOD1* during *Sclerotinia sclerotiorum* inoculation. **Figure S2.** Phylogenetic relationship of the CCS and SOD genes in *S. sclerotiorum* and *Arabidopsis thaliana*. **a** Phylogenetic relationship of the *S. sclerotiorum* CCS (*SS1G_00102*) and the *A. thaliana* CCS (*AT1G12520*). **b** Phylogenetic relationship of the *S. sclerotiorum* SOD (*SS1G_00699*) and the *A. thaliana* SOD genes (*AT2G28190*, *AT5G18100*, *AT1G08830*). **Figure S3.** Sequence alignment of *S. sclerotiorum SsCCS* and *SsSOD* with *A. thaliana AtCCS* and *AtSOD1*. The black horizontal lines in the *S. sclerotiorum* gene indicate the sequences used to construct host-induced gene silencing (HIGS) vectors. **Figure S4.** Comparison of growth between transgenic and control *A. thaliana* lines. **Figure S5.** Relative expression levels of *AtCCS* and *AtSOD1* in transgenic HIGS plants. The expression levels were quantified by normalizing the quantity of *A. thaliana AtActin7* and *AtActin2* cDNA in different samples. Data are presented as means ± SEM (n = 3, technical replicates). The same letter indicates no statistically significant difference at $p > 0.05$ (two-sided Student's *t*-test). The relative expression of the target gene in CK was set as one, respectively. CK: *A. thaliana* plants carrying the empty vector.

Additional file 2: Table S1. Information on the primers used in this study.

Acknowledgements

The authors thank Prof. Yang Yu (Southwest University) and Prof. Chunyu Zhang (Huazhong Agricultural University) for providing vectors and yeast strains used in this study.

Author contributions

Yijuan Ding and Wei Qian designed and supervised this research. Yijuan Ding and Baoqin Yan designed the experiments for transgenic lines. Baoqin Yan and Siqi Zhao designed the experiments for the ROS detection. Yijuan Ding, Baoqin Yan, and Yangui Chen managed the resistance assay. Yijuan Ding, Baoqin Yan, and Huafang Wan performed the data analysis. Yijuan Ding and Wei Qian prepared the manuscript.

Funding

This study received financial support from the National Natural Science Foundation of China (31971978 and 32072021), the Natural Science Foundation of Chongqing (CSTB2023NSCQ-MSX0355), the Fundamental Research Funds for the Central Universities (SWU120075), and the Youth Science and Technology Fund of Gansu Province (23JRRL0005).

Availability of data and materials

The data supporting the findings of this study are available from the corresponding author upon reasonable request.

Declarations

Ethics approval and consent to participate

Not applicable.

Consent for publication

Not applicable.

Competing interests

The authors declare that they have no competing interests.

Received: 13 December 2023 Accepted: 1 March 2024
Published online: 16 April 2024

References

Andrade CM, Tinoco MLP, Rieth AF, Maia FCO, Aragão FJL. Host-induced gene silencing in the necrotrophic fungal pathogen *Sclerotinia sclerotiorum*. Plant Pathol. 2015;65:626–32.

Banci L, Bertini I, Cantini F, Kozyreva T, Massagni C, Palumaa P, et al. Human superoxide dismutase 1 (hSOD1) maturation through interaction with human copper chaperone for SOD1 (hCCS). Proc Natl Acad Sci U S A. 2012;109:13555–60.

Bi G, Hu M, Fu L, Zhang X, Zuo J, Li J, et al. The cytosolic thiol peroxidase PRXIIB is an intracellular sensor for H_2O_2 that regulates plant immunity through a redox relay. Nat Plants. 2022;8:1160–75.

Boller T, Felix G. A renaissance of elicitors: perception of microbe-associated molecular patterns and danger signals by pattern-recognition receptors. Annu Rev Plant Biol. 2009;60:379–406.

Bolton MD, Thomma BPHJ, Nelson BD. Sclerotinia sclerotiorum (Lib.) de Bary: biology and molecular traits of a cosmopolitan pathogen. Mol Plant Pathol. 2006;7:1–16.

Cai Q, Qiao L, Wang M, He B, Lin FM, Palmquist J, et al. Plants send small RNAs in extracellular vesicles to fungal pathogen to silence virulence genes. Science. 2018;360:1126–9.

Chai M, Fan R, Huang Y, Jiang X, Wai MH, Yang Q, et al. GmbZIP152, a soybean bZIP transcription factor, confers multiple biotic and abiotic stress responses in plant. Int J Mol Sci. 2022;23:10935.

Clough SJ, Bent AF. Floral dip: a simplified method for Agrobacterium-mediated transformation of *Arabidopsis thaliana*. Plant J. 1998;16:735–43.

Delaunay A, Pflieger D, Barrault MB, Vinh J, Toledano MB. A thiol peroxidase is an H_2O_2 receptor and redox-transducer in gene activation. Cell. 2002;111:471–81.

Ding Y, Mei J, Chai Y, Yang W, Mao Y, Yan B, et al. *Sclerotinia sclerotiorum* utilizes host-derived copper for ROS detoxification and infection. PLoS Pathog. 2020;16: e1008919.

Ding Y, Chen Y, Yan B, Liao H, Dong M, Meng X, et al. Host-induced gene silencing of a multifunction gene Sscnd1 enhances plant resistance against *Sclerotinia sclerotiorum*. Front Microbiol. 2021;12: 693334.

El Hadrami A, El Idrissi-Tourane A, El Hassni M, Daayf F, El Hadrami I. Toxin-based in-vitro selection and its potential application to date palm for resistance to the bayoud Fusarium wilt. C R Biol. 2005;328:732–44.

Jones JD, Dangl JL. The plant immune system. Nature. 2006;444:323–9.

Kabbage M, Williams B, Dickman MB. Cell death control: the interplay of apoptosis and autophagy in the pathogenicity of *Sclerotinia sclerotiorum*. PLoS Pathog. 2013;9: e1003287.

Kiselev KV, Aleynova OA, Ogneva ZV, Suprun AR, Dubrovina AS. 35S promoter-driven transgenes are variably expressed in different organs of *Arabidopsis thaliana* and in response to abiotic stress. Mol Biol Rep. 2021;48:2235–41.

Koubaa S, Brini F. Functional analysis of a wheat group 3 late embryogenesis abundant protein (TdLEA3) in Arabidopsis thaliana under abiotic and biotic stresses. Plant Physiol Biochem. 2020;156:396–406.

Kumar D, Yusuf MA, Singh P, Sardar M, Sarin NB. Histochemical detection of superoxide and H_2O_2 accumulation in *Brassica juncea* seedlings. Bio-Protoc. 2014;4: e1108.

Liang X, Rollins JA. Mechanisms of broad host range necrotrophic pathogenesis in *Sclerotinia sclerotiorum*. Phytopathology. 2018;108:1128–40.

Lin L, Fan J, Li P, Liu D, Ren S, Lin K, et al. The *Sclerotinia sclerotiorum*-inducible promoter pBnGH17D7 in *Brassica napus*: isolation, characterization and application in host-induced gene silencing. J Exp Bot. 2022;73:6663–77.

Liu D, Wu J, Lin L, Li P, Li S, Wang Y, et al. Overexpression of Cinnamoyl-CoA reductase 2 in *Brassica napus* increases resistance to *Sclerotinia sclerotiorum* by affecting lignin biosynthesis. Front Plant Sci. 2021;12: 732733.

Livak KJ, Schmittgen TD. Analysis of relative gene expression data using real-time quantitative PCR and the $2^{-\Delta\Delta CT}$ method. Methods. 2001;25:402–8.

López-Cruz J, Óscar CS, Emma FC, Pilar GA, Carmen GB. Absence of Cu-Zn superoxide dismutase BCSOD1 reduces *Botrytis cinerea* virulence in Arabidopsis and tomato plants, revealing interplay among reactive oxygen species, callose and signalling pathways. Mol Plant Pathol. 2017;18:16–31.

Lyu X, Shen C, Fu Y, Xie J, Jiang D, Li G, et al. A small secreted virulence-related protein is essential for the necrotrophic interactions of *Sclerotinia sclerotiorum* with its host plants. PLoS Pathog. 2016;12: e1005435.

Mahto BK, Singh A, Pareek M, Rajam MV, Dhar-Ray S, Reddy PM. Host-induced silencing of the *Colletotrichum gloeosporioides* conidial morphology 1 gene (*CgCOM1*) confers resistance against Anthracnose disease in chilli and tomato. Plant Mol Biol. 2020;104:381–95.

Maximiano MR, Santos LS, Santos C, Aragão FJL, Dias SC, Franco OL, et al. Host induced gene silencing of *Sclerotinia sclerotiorum* effector genes for the control of white mold. Biocatal Agric Biotechnol. 2022;40: 102302.

McCaghey M, Shao D, Kurcezewski J, Lindstrom A, Ranjan A, Whitham SA, et al. Host-induced gene silencing of a *Sclerotinia sclerotiorum* oxaloacetate acetylhydrolase using bean pod mottle virus as a vehicle reduces disease on soybean. Front Plant Sci. 2021;12: 677631.

Mittler R, Vanderauwera S, Suzuki N, Miller G, Tognetti VB, Vandepoele K, et al. ROS signaling: the new wave? Trends Plant Sci. 2011;16:300–9.

Mittler R. ROS are good. Trends Plant Sci. 2017;22:11–9.

Oparka M, Walczak J, Malinska D, van Oppen LMPE, Szczepanowska J, Koopman WJH, et al. Quantifying ROS levels using CM-H_2DCFDA and HyPer. Methods. 2016;109:3–11.

Peng KC, Lin CC, Liao CF, Yu HC, Lo CT, Yang HH, et al. Expression of L-amino acid oxidase of *Trichoderma harzianum* in tobacco confers resistance to *Sclerotinia sclerotiorum* and *Botrytis cinerea*. Plant Sci. 2021;303: 110772.

Rana K, Yuan J, Liao H, Banga SS, Kumar R, Qian W, et al. Host-induced gene silencing reveals the role of *Sclerotinia sclerotiorum* oxaloacetate acetylhydrolase gene in fungal oxalic acid accumulation and virulence. Microbiol Res. 2022;258: 126981.

Segal LM, Wilson RA. Reactive oxygen species metabolism and plant-fungal interactions. Fungal Genet Biol. 2018;110:1–9.

Shao HB, Chu LY, Lu ZH, Kang CM. Primary antioxidant free radical scavenging and redox signaling pathways in higher plant cells. Int J Biol Sci. 2007;4:8–14.

Shen BR, Wang LM, Lin XL, Yao Z, Xu HW, Zhu CH, et al. Engineering a new chloroplastic photorespiratory bypass to increase photosynthetic efficiency and productivity in rice. Mol Plant. 2019;12:199–214.

Sies H, Berndt C, Jones DP. Oxidative stress. Annu Rev Biochem. 2017;86:715–48.

Singh Y, Nair AM, Verma PK. Surviving the odds: From perception to survival of fungal phytopathogens under host-generated oxidative burst. Plant Commun. 2021;2: 100142.

Tang L, Yang G, Ma M, Liu X, Li B, Xie J, et al. An effector of a necrotrophic fungal pathogen targets the calcium-sensing receptor in chloroplasts to inhibit host resistance. Mol Plant Pathol. 2020;21:686–701.

Tian L, Li J, Huang C, Zhang D, Xu Y, Yang X, et al. Cu/Zn superoxide dismutase (VdSOD1) mediates reactive oxygen species detoxification and modulates virulence in *Verticillium dahliae*. Mol Plant Pathol. 2021;22:1092–108.

Veluchamy S, Williams B, Kim K, Dickman M. The CuZn superoxide dismutase from *Sclerotinia sclerotiorum* is involved with oxidative stress tolerance, virulence, and oxalate production. Physiol Mol Plant Pathol. 2012;78:14–23.

Verma R, Kaur J. Expression of barley oxalate oxidase confers resistance against *Sclerotinia sclerotiorum* in transgenic *Brassica juncea* cv *varuna*. Transgenic Res. 2021;30:143–54.

Wang LM, Shen BR, Li BD, Zhang CL, Lin M, Tong PP, et al. A synthetic photorespiratory shortcut enhances photosynthesis to boost biomass and grain yield in rice. Mol Plant. 2020a;13:1802–15.

Wang Z, Bao LL, Zhao FY, Tang MQ, Chen T, Li Y, et al. BnaMPK3 is a key regulator of defense responses to the devastating plant pathogen *Sclerotinia sclerotiorum* in oilseed rape. Front Plant Sci. 2019;10:91.

Wang Z, Wan L, Zhang X, Xin Q, Song Y, Hong D, et al. Interaction between *Brassica napus* polygalacturonase inhibition proteins and *Sclerotinia sclerotiorum* polygalacturonase: implications for rapeseed resistance to fungal infection. Planta. 2021;253:34.

Wang Z, Zhao FY, Tang MQ, Chen T, Bao LL, Cao J, et al. BnaMPK6 is a determinant of quantitative disease resistance against *Sclerotinia sclerotiorum* in oilseed rape. Plant Sci. 2020b;291: 110362.

Waszczak C, Carmody M, Kangasjärvi J. Reactive oxygen species in plant signaling. Annu Rev Plant Biol. 2018;69:209–36.

Wei W, Xu L, Peng H, Zhu W, Tanaka K, Cheng J, et al. A fungal extracellular effector inactivates plant polygalacturonase-inhibiting protein. Nat Commun. 2022;13:2213.

Williams B, Kabbage M, Kim HJ, Britt R, Dickman MB. Tipping the balance: *Sclerotinia sclerotiorum* secreted oxalic acid suppresses host defenses by manipulating the host redox environment. PLoS Pathog. 2011;7: e1002107.

Wu J, Yin S, Lin L, Liu D, Ren S, Zhang W, et al. Host-induced gene silencing of multiple pathogenic factors of *Sclerotinia sclerotiorum* confers resistance to Sclerotinia rot in *Brassica napus*. CROP J. 2022;10:661–71.

Xu L, Chen W. Random T-DNA Mutagenesis Identifies a Cu/Zn superoxide dismutase gene as a virulence factor of *Sclerotinia sclerotiorum*. Mol Plant Microbe in. 2013;26:431–41.

Xu G, Yuan M, Ai C, Liu L, Zhuang E, Karapetyan S, et al. uORF-mediated translation allows engineered plant disease resistance without fitness costs. Nature. 2017;545:491–4.

Yan J, Wang X. Machine learning bridges omics sciences and plant breeding. Trends Plant Sci. 2023;28:199–210.

Yang G, Tang L, Gong Y, Xie J, Fu Y, Jiang D, et al. A cerato-platanin protein SsCP1 targets plant PR1 and contributes to virulence of *Sclerotinia sclerotiorum*. New Phytol. 2018;217:739–55.

Yang X, Yang J, Wang Y, He H, Niu L, Guo D, et al. Enhanced resistance to sclerotinia stem rot in transgenic soybean that overexpresses a wheat oxalate oxidase. Transgenic Res. 2019;28:103–14.

Yao SH, Guo Y, Wang YZ, Zhang D, Xu L, Tang WH. A cytoplasmic Cu-Zn superoxide dismutase SOD1 contributes to hyphal growth and virulence of *Fusarium graminearum*. Fungal Genet Biol. 2016;91:32–42.

Yuan M, Jiang Z, Bi G, Nomura K, Liu M, Wang Y, et al. Pattern-recognition receptors are required for NLR-mediated plant immunity. Nature. 2021;592:105–9.
Zhang M, Liu Y, Li Z, She Z, Chai M, Aslam M, et al. The bZIP transcription factor GmbZIP15 facilitates resistance against *Sclerotinia sclerotiorum* and *Phytophthora sojae* infection in soybean. Iscience. 2021;24:102642.
Zhang T, Zhao YL, Zhao JH, Wang S, Jin Y, Chen ZQ, et al. Cotton plants export microRNAs to inhibit virulence gene expression in a fungal pathogen. Nat Plants. 2016;2:16153.
Zhao Y, Zhu X, Chen X, Zhou JM. From plant immunity to crop disease resistance. J Genet Genomics. 2022;49:693–703.
Zhu W, Wei W, Fu Y, Cheng J, Xie J, Li G, et al. A secretory protein of necrotrophic fungus *Sclerotinia sclerotiorum* that suppresses host resistance. PLoS ONE. 2013;8: e53901.